18A

PNL-4001-7
UC-90g

Development of Materials for Open-Cycle MHD

Quarterly Report for the Period Ending March 1984

D. D. Marchant
J. L. Bates

September 1984

Prepared for the U.S. Department of Energy
under Contract DE-AC06-76RLO 1830

Pacific Northwest Laboratory
Operated for the U.S. Department of Energy
by Battelle Memorial Institute

Battelle

PNL-4001-7

DISCLAIMER

PACIFIC NORTHWEST LABORATORY
operated by
BATTELLE
for the
UNITED STATES DEPARTMENT OF ENERGY
under Contract DE-AC06-76RLO 1830

Printed in the United States of America
Available from
National Technical Information Service
United States Department of Commerce
5285 Port Royal Road
Springfield, Virginia 22161

NTIS Price Codes
Microfiche A01

Printed Copy

Pages	Price Codes
001-025	A02
026-050	A03
051-075	A04
076-100	A05
101-125	A06
126-150	A07
151-175	A08
176-200	A09
201-225	A010
226-250	A011
251-275	A012
276-300	A013

PNL-4001-7
UC-90g

DEVELOPMENT OF MATERIALS FOR OPEN-CYCLE MHD

Quarterly Report for the Period
Ending March 1984

D. D. Marchant
J. L. Bates

September 1984

Prepared for
the U.S. Department of Energy
under Contract DE-AC06-76RLO 1830

Pacific Northwest Laboratory
Richland, Washington 99352

SUMMARY

Pacific Northwest Laboratory (PNL) is conducting a study of channel components for open-cycle, coal-fired magnetohydrodynamic (MHD) generators. Specifically, electrodes and insulators are being developed. The electrical conductivity has been measured on several compositions based on indium oxide-tin oxide (In_2O_3-SnO_2). These compositions have been studied as additives to refractory ceramic oxides to increase the low-temperature electrical conductivity. Indium oxide appears to be the main constituent required for high conductivity. The electrical conductivity of In_2O_3-SnO_2 compositions increases with increasing In_2O_3 concentration and reaches a maximum with compositions containing about 95 mol% In_2O_3. These high In_2O_3-containing compositions behave like degenerate semiconductors; the electrical conductivity decreases with increasing temperature. Three major crystallographic phases were identified for each composition, and were tested for their relative electrical conductivity and corrosion resistance to determine which phase would be most suitable for use as an additive to refractory ceramic oxides.

CONTENTS

FIGURES

TABLE

INTRODUCTION

Pacific Northwest Laboratory (PNL)[a] is developing and testing ceramic electrodes and insulators and other channel components for open-cycle, coal-fired magnetohydrodynamic (MHD) generators as part of the U.S. Department of Energy (DOE) Power Generation Program. The objectives of the PNL program are to develop:

- electrodes that can withstand the severe corrosive and erosive environment of an MHD channel and that will transfer electrical current efficiently during long channel operation
- insulators that can withstand the corrosive and erosive environment and maintain adequate electrical resistivity during long channel operation
- electrode and insulator designs that are compatible with the demands of channel assembly, operation, and disassembly.

The program is divided into four tasks:

- development and fabrication of electrodes/insulators
- design and testing of electrodes/insulators
- characterization and evaluation of electrode/insulator materials
- measurement of thermal, electrical, and mechanical properties.

Because the tasks are interrelated, the quarterly reports for this program are organized by activities and not necessarily by specific tasks. This report will describe the fabrication procedures and discuss the electrical conductivity and corrosion properties of several In_2O_3-SnO_2 compositions.

(a) Operated for the U.S. Department of Energy by Battelle Memorial Institute.

TECHNICAL PROGRESS

Several compositions of indium oxide-tin oxide (In_2O_3-SnO_2), in addition to those reported previously (Marchant and Bates 1983b), have been fabricated and the electrical conductivity has been measured. Some of the results have been included in a paper that has been accepted for publication and presentation at the Symposium on Engineering Aspects of Magnetohydrodynamics (SEAM) (Marchant 1984). Since these materials appear to be useful to other energy conversion systems, some of the data were also included in a report to the DOE as part of the DOE-Advanced Research and Technology Development (ARTD) efforts (Bates and Marchant 1984a,b).

POWDER PREPARATION AND FABRICATION

The In_2O_3-SnO_2 compositions were prepared by sintering coprecipitated powders. The coprecipitation technique was a modification of that used by Dole et al. (1978). Indium oxide and a suboxide of tin (SnO) were dissolved in hot nitric acid.

The nitric acid solutions were mixed and diluted with distilled water to about 10 times the volume. The resulting solution was slowly dripped into ammonium hydroxide, which had been diluted to two times the volume with water. The final pH was adjusted to between 8.0 and 8.5 to ensure complete precipitation.

The resulting precipitate was washed sequentially with water, acetone, toluene, and acetone again, then air-dried, and finally calcined at 1073K for 5 h. The resulting powder had a surface area ranging between 5 and 25 m^2/g (BET equation using argon). The powder was then ball milled for 16 h using magnesium-stabilized zirconium oxide balls in a neoprene-lined ball mill with Freon® TF liquid.

The powder was compacted into rectangular bars using cold pressing in steel dies followed by isostatic pressing. The compacted bars were sintered in

® Trademark of E. I. du Pont de Nemours and Company, Inc., Wilmington, Delaware.

air for 20 h at temperatures between 1800K and 1850K, and were then cut with a diamond saw into the shapes for testing. The samples were then examined, using both x-ray diffraction and scanning electron microscopy with energy-dispersive x-ray analysis (SEM-EDX), to identify the major crystallographic phases.

The x-ray diffraction used Cu-Kα x-rays that were first passed through a diffracted-beam monochrometer; the phases identified by this method are listed in Table 1. The three principal phases, illustrated in Figure 1, are:

- a tetragonal phase containing mostly SnO_2; the unit cell has lattice parameters of $a_o \sim 47.3$ nm and $C_o \sim 31.8$ nm (Figure 1a)
- a rhombohedral phase that is a distortion of a cubic fluorite; this phase contains nearly equal amounts of In_2O_3 and SnO_2 and has a structure that is commonly labeled "Tb_7O_{12}" (Wells 1975); the unit cell has lattice parameters of $a_o \sim 80.0$ nm and a 7.3° angle (Figure 1b)
- a body-centered-cubic (bcc) phase containing mostly In_2O_3; the unit cell has a lattice parameter of $a_o \sim 101.4$ nm (Figure 1c).

The relative amounts of each phase (expressed as weight percent) are estimated from x-ray diffraction peak heights; the values could vary by as much as ±5 percentage points. The phases in the table show a smooth progression of phases from mostly tetragonal (in the samples containing large amounts of SnO_2) through mostly rhombohedral (where the amounts of In_2O_3 and SnO_2 are nearly equal) to mostly bcc (in samples containing large amounts of In_2O_3).

The fabrication process produced sintered bars with densities from 70% to 95% of theoretical (%TD). The higher-density samples were those with higher In_2O_3 concentrations. Commercial production of SnO_2 electrodes usually involves the use of additives to promote sintering by formation of liquid phases along the grain boundaries. The addition of In_2O_3 to SnO_2 resulted in greater sintering densities. The In_2O_3 therefore acted as a sintering aid, although no evidence was observed of a liquid phase at the grain boundary.

TABLE 1. Electrical Conductivity and Phase Equilibria for the In_2O_3-SnO_2 Compositions Shown in Figure 2

Composition, mol%		Electrical Conductivity,[a] $ohm^{-1}\ cm^{-1}$		Activation Energy, eV	Temperature Range, K	Phases Present,[b] wt%
In_2O_3	SnO_2	A	B			
7	93	(c)	(c)	(c)	<1111	80 T
		6.814	11.090×10^3	2.20	1111 to 1726	20 R
11	89	0.015	8.230×10^2	0.16	524 to 1029	50 T
		3.659	4.573×10^3	0.91	1029 to 1720	50 R
16	84	1.409	1.155×10^3	0.23	606 to 961	60 T
		(c)	(c)	(c)	>961	40 R
23	77	1.945	1.232×10^3	0.24	308 to 930	40 T
		3.977	3.121×10^3	0.62	930 to 1433	60 R
		(c)	(c)	(c)	1433 to 1732	
31	69	3.086	1.210×10^3	0.24	847 to 1148	25 T
		(c)	(c)	(c)	>1148	75 R
38	59	2.00[d]	(d)	(d)	<1000	5 T
		3.1106	1.116×10^3	0.22	1000 to 1738	95 R
						Trace bcc
50	50	2.086	5.214×10	0.010	678 to 1052	90 R
		2.961	9.253×10^2	0.18	1052 to 1626	10 bcc
54	46	2.93	2.46×10^2	0.05	702 to 1358	80 R
		3.982	1.672×10^3	0.33	1358 to 1725	20 bcc
60	40	2.212	-1.908×10^2	-0.038[e]	678 to 1016	40 R
		3.262	8.760×10^2	0.17	1016 to 1625	60 bcc
60	40	2.353	-1.134×10^2	-0.023[e]	689 to 1042	40 R
		3.168	7.366×10^2	0.15	1042 to 1632	60 bcc
70	30	2.695	-1.037×10^2	-0.021[e]	587 to 1118	10 R
		3.174	4.319×10^2	0.086	1118 to 1506	90 bcc
80	20	3.04	-7.582×10	-0.015[e]	585 to 1578	5 R
						95 bcc
90	10	2.624	-2.943×10	-0.006[e]	746 to 1720	Trace R
						100 bcc
95	5	3.276	-7.313×10	-0.015[e]	485 to 1543	100 bcc
100	0	1.752	-1.551×10^2	-0.03[e]	401 to 1631	100 bcc

(a) $\text{Log}_{10}\ \sigma = A - BT^{-1}$ where T is in Kelvin.
(b) T = tetragonal; R = rhombohedral; bcc = body-centered cubic.
(c) Nonlinear.
(d) Nearly temperature independent.
(e) Positive slope.

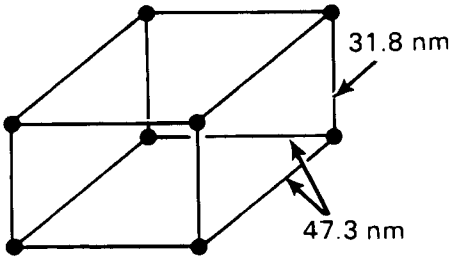

a) Tetragonal

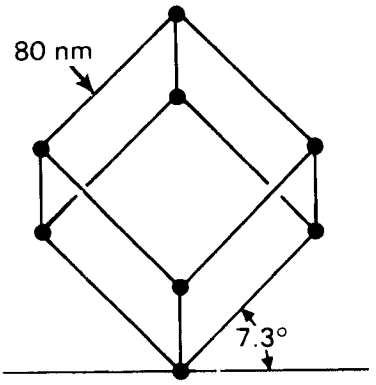

b) Rhombohedral

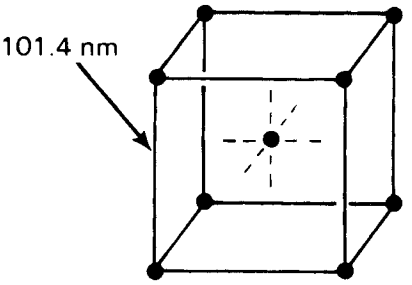

c) Body-Centered Cubic

FIGURE 1. Crystal Structure of Major Crystallographic Phases of In_2O_3-SnO_2 Compositions

ELECTRICAL CONDUCTIVITY

The electrical conductivity of the samples was measured to 1700K in air using the four-contact direct-current method described previously (Marchant and Bates 1983a). The test samples were rectangular with a square cross section. The electrodes were platinum, and platinum paste was used to provide a high-conductivity interface between the electrode and the test sample. Direct electric currents with densities not exceeding 0.05 A/cm^2 were passed through the sample. The electric potential along the sample was measured using platinum knife-edge probes. Ohm's law was used to calculate the resistivity.

The results of the conductivity measurements are shown in Figure 2. Conductivity is expressed in units of Siemens per centimeter (S/cm) where $S = mho = ohm^{-1}$. The In_2O_3 concentration (expressed in mol%) is shown for each curve. Shown are the actual data points as well as the curves resulting from a

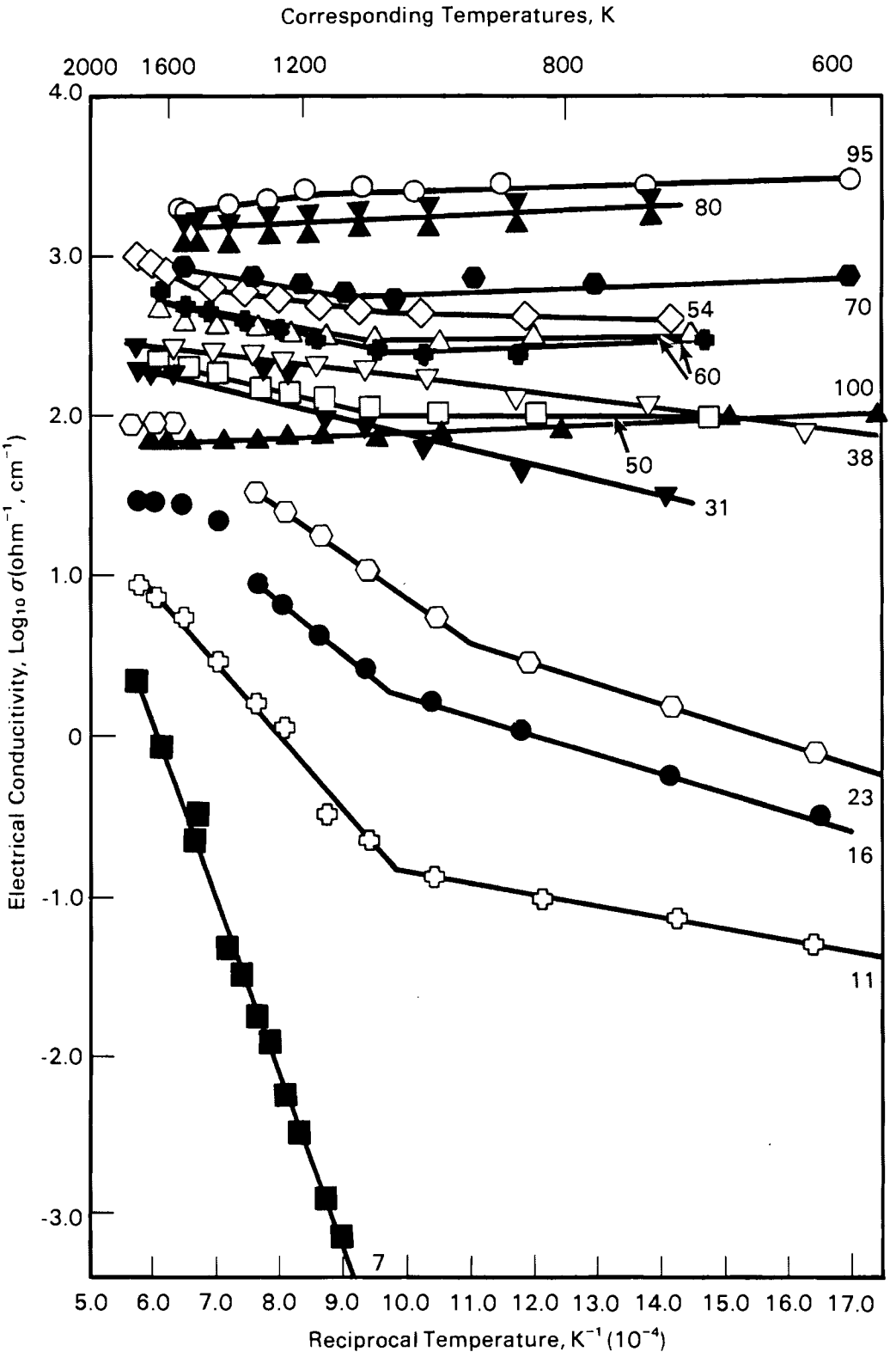

FIGURE 2. Electrical Conductivity As a Function of Temperature for Several In_2O_3-SnO_2 Samples

least-squares curve fit. The accuracy of fit, expressed as a coefficient of determination, was greater than 0.95 for each of the curves. The figure includes data reported previously (Marchant and Bates 1983b).

Electrical conductivity increases as the indium content increases. The amount of increase is greatest with In_2O_3 concentrations between 7 and 31 mol%. At greater In_2O_3 concentrations, the amount of increase is much smaller. The maximum conductivity is attained with an In_2O_3 concentration around 95 mol%, and is a factor of about 10 greater than pure In_2O_3. The conductivity mechanisms have not been studied, but preliminary measurements of the Seebeck coefficient show that the material is an n-type semiconductor. Relating this coefficient to the electrical conductivity indicates that some of the measured compositions were degenerate semiconductors. A degenerate semiconductor has the Fermi level in the conduction band; consequently, the number of electrons found in this band is close to that in metals, and the conductivity should resemble that of a metal. Metallic conduction decreases with increases in temperature, as was found in several of the In_2O_3-SnO_2 compositions with In_2O_3 concentrations greater than 60 mol%. This type of electrical conductivity would be ideal for MHD generator channels because 1) the conduction is electronic so that ions would not migrate and 2) the low temperature dependence of the conductivity would lead to electrical stability of the electrode and reduce the possibility of current channeling. Unfortunately, In_2O_3-SnO_2 compositions are not resistant to slag and molten salt corrosion; therefore, they cannot be used directly as either the refractory cap or the current leadout. However, they can be added to other ceramic materials to make them more conductive.

Most of the electrical conductivity data shown in Figure 2 can be expressed in the form of the following equation:

$$\mathrm{Log}_{10}\,\sigma = A - \frac{B}{T} \qquad (1)$$

where A and B are constants and T is the temperature in Kelvin.

The temperature dependence of the conductivity is given by the constant B. A positive B value indicates that the conductivity increases with temperature

and a negative value indicates a decrease with temperature. Multiplying the B value by 1.986×10^{-4} results in the temperature dependence, expressed in electron volts (eV). Table 1 presents the A and B values for the equations for the curves shown in Figure 2, the temperature dependence of the conductivity, and the range of temperatures for which the equations are useful. Conductivity data for compositions with low concentrations of In_2O_3 are described by two equations; compositions with higher concentrations of In_2O_3 are described by one equation. For the compositions with higher concentrations of In_2O_3, the temperature dependence is negative, resulting in a decrease in conductivity with increasing temperature (see Figure 2). The development of the bcc phase is parallel with the electrical conductivity becoming more independent of temperature. The lowest electrical conductivity and the greatest temperature dependence are found with the tetragonal phase. Included in Table 1 are revised equations for the data reported previously (Marchant and Bates 1983b).

The electrical conductivity of In_2O_3-SnO_2 is compared with other materials (including metals, non-oxide ceramics, coal slag, and seeded MHD combustion gases) in Figure 3. The shaded band in the figure represents In_2O_3-SnO_2 compositions ranging from 41 to 95 mol% In_2O_3. The In_2O_3-SnO_2 conductivity is within several orders of magnitude of the conductivity of metals such as platinum and copper. Adding these highly conducting ceramics to the hafnium oxide/rare earth oxide compositions should significantly increase the electrical conductivity of these oxides.

CORROSION TESTING

The corrosion tests did not use electric fields; consequently, only chemical rather than electrochemical corrosion was examined. The chemical corrosion tests are adequate for the initial screening. The In_2O_3-SnO_2 compositions are not sufficiently corrosion resistant and therefore will not be used directly for current leadouts but will be mixed with other, more corrosion-resistant materials. Electrochemical corrosion tests will be used later on the compositions resulting from the addition of In_2O_3-SnO_2 to the

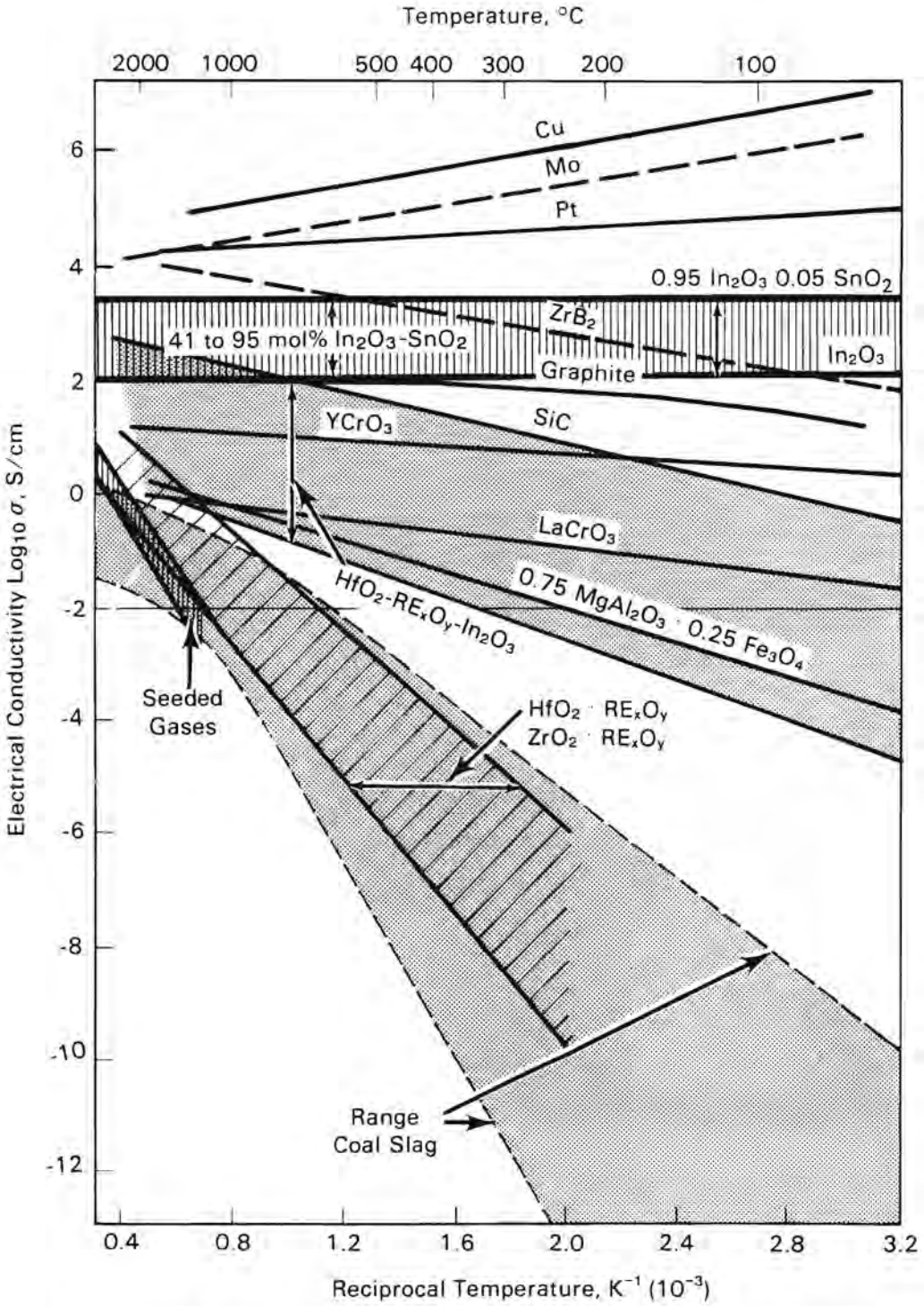

FIGURE 3. Electrical Conductivity of Several Materials

HfO_2-RE_xO_y compositions, which are more corrosion resistant. Corrosion tests were conducted in two types of media: 1) K_2SO_4 at 1373K and 2) Montana Rosebud coal slag at 1723K.

The corrosion tests consisted of immersing the rectangular test samples in the medium for a predetermined time, usually between 24 and 96 h. In the molten salt tests, the samples were removed and cooled; the surface molten salt was removed by washing in dilute nitric acid. The sample dimensions were measured and the samples were either reimmersed in the molten salt for continued testing or were prepared metallographic examination. In the slag tests, the samples were cooled in the slag. The sample and slag were then metallographically examined. Figure 4 shows several optical micrographs of the sample/slag interface. All tests were conducted in an air atmosphere.

The molten salt corrosion tests indicated that the bcc phase (mostly In_2O_3) was the most corrodible phase. The rhombohedral and the tetragonal phases were more corrosion resistant.

Corrosion in molten coal slag was more extensive than in molten salt. High temperatures and the existence of many corrosive species in the silicates contributed to the increased corrosion. In these tests, the bcc phase appeared to be the most corrodible, followed by the rhombohedral phase; the tetragonal phase was the least corrodible.

A sample containing 10 wt% bcc and 90 wt% rhombohedral phase had a chemical composition of 50 mol% In_2O_3 and 50 mol% SnO_2. The rhombohedral phase contained 44 mol% In_2O_3 and 56 mol% SnO_2. The stoichiometric ratio for the rhombohedral phase should be 40 mol% In_2O_3 and 60 mol% SnO_2. The additional rhombohedral-phase In_2O_3 was due to its being in equilibrium with the bcc In_2O_3 phase. The remainder of the In_2O_3 was found in the bcc phase, which had a composition of 88 mol% In_2O_3 and 12 mol% SnO_2. The main slag attack occurred in the bcc phase, resulting in the solution of this phase into the slag. The secondary attack was in the rhombohedral phase. Leaching of some of the indium in that phase resulted in the composition becoming richer in SnO_2. As indium was leached, the tetragonal phase formed. The solubility of In_2O_3 in the

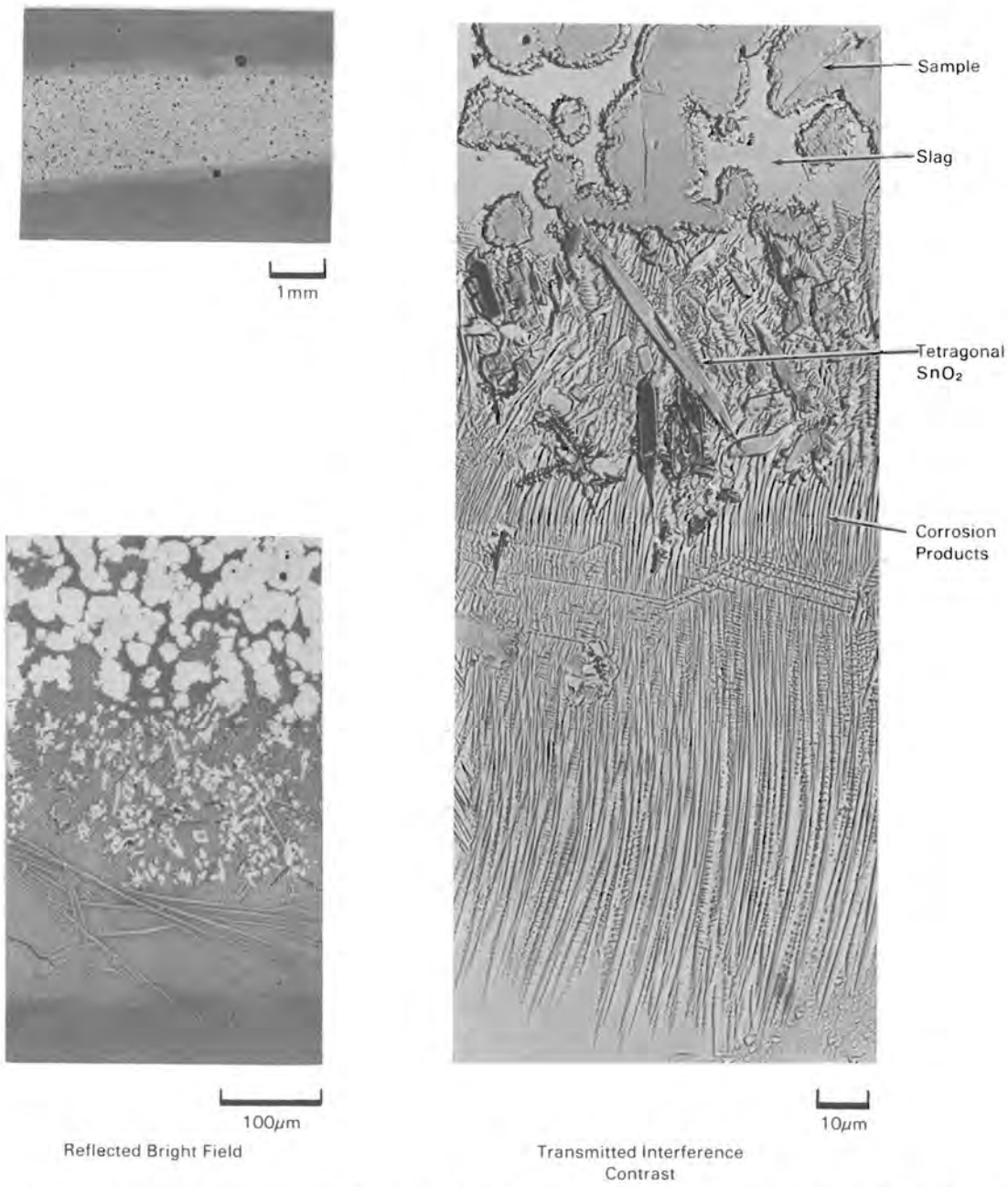

FIGURE 4. Optical Micrographs of the Interface Between In_2O_3-SnO_2 and Coal Slag. Reflected light bright field and transmitted interference contrast are shown.

tetragonal phase was about 11 mol%. The tertiary attack occurred at the grain boundaries. This attack freed some of the grains from the ceramic and they went into the bulk slag. The secondary and tertiary attacks occurred at such rates that the tetragonal phase materials were found in the coal slag. These grains continued to lose In_2O_3 until the tetragonal phase contained only 1 or 2 mol% In_2O_3, which is less than the solubility limit. The SnO_2 phase has a very low solubility for slag components, as evidenced by the lack of such components measured in the SEM-EDX analysis.

Unfortunately, the tetragonal phase does not have high electrical conductivity. Therefore, the best composition to add to a refractory ceramic may be one that contains the rhombohedral phase to increase the electrical conductivity and still to maintain some corrosion resistance. This composition will be around 40 mol% In_2O_3 and 60 mol% SnO_2. Future studies will be required to determine whether the additive will produce sufficiently high conductivity.

CONCLUSIONS AND RECOMMENDATIONS

Compositions based on In_2O_3-SnO_2 were fabricated by sintering coprecipitated powders. The resulting densities ranged between 70 and 95 %TD. The higher densities were associated with higher concentrations of In_2O_3.

The electrical conductivity was measured in air for each of these compositions. The conductivity is n-type and for In_2O_3 concentrations greater than 60 mol% indicates that the materials are degenerate semiconductors. The temperature dependence of electrical conductivity generally decreases with increasing In_2O_3 concentrations. At In_2O_3 concentrations greater than 70 mol%, the temperature dependence becomes negative, indicating a decrease in the conductivity with an increase in temperature.

Three phases were identified in the In_2O_3-SnO_2 compositions: 1) a tetragonal phase containing mostly SnO_2, 2) a rhombohedral phase containing nearly equal amounts of SnO_2 and In_2O_3, and 3) a bcc phase containing mostly In_2O_3. The bcc phase appears to have the greatest electrical conductivity and the least corrosion resistance in both molten K_2SO_4 and Montana Rosebud coal slag. The tetragonal phase has the lowest conductivity and the greatest corrosion resistance. The rhombohedral phase appears to be the best compromise, having intermediate conductivity and corrosion resistance. It is therefore recommended that this phase be added to the HfO_2-RE_xO_y refractory oxides to increase conductivity.

Future activities will include fabrication of HfO_2-RE_xO_y- In_2O_3-SnO_2 compositions having an In_2O_3-to-SnO_2 ratio of 2 to 3. This ratio gives the rhombohedral phase. The electrical conductivity of these compositions will be measured. The compositions will also be tested for chemical corrosion resistance in molten coal slags.

REFERENCES

Bates, J. L., and D. D. Marchant. 1984a. "Oxide Electrodes for High-Temperature Fuel Cells." In Fossil Energy Materials Program Quarterly Report for the Period Ending December 31, 1983. ORNL/FMP-84-1, Oak Ridge National Laboratory, Oak Ridge, Tennessee.

Bates, J. L., and D. D. Marchant. 1984b. In Fossil Energy Materials Program Quarterly Report for the Period Ending March 31, 1984. ORNL/FMP-84-2, Oak Ridge National Laboratory, Oak Ridge, Tennessee.

Dole, S. L., et al. 1978. "Technique for Preparing Highly Sinterable Oxide Powders." Mat. Sci. Engr. 32:277-281.

Marchant, D. D. 1984. "Ceramic Materials for MHD Electrodes." In Proceedings of the 22nd Symposium on the Engineering Aspects of MHD, June 26-28, 1984, Mississippi State University, Mississippi State, Mississippi.

Marchant, D. D., and J. L. Bates. 1983a. Development of Materials for Open-Cycle MHD - Quarterly Report for the Period Ending December 1982. PNL-4001-2, Pacific Northwest Laboratory, Richland, Washington.

Marchant, D. D., and J. L. Bates. 1983b. Development of Materials for Open-Cycle MHD - Quarterly Report for the Period Ending June 1983. PNL-4001-4, Pacific Northwest Laboratory, Richland, Washington.

Wells, A. F. 1975. Structural Inorganic Chemistry. Clarendon Press, Oxford.

DISTRIBUTION

No. of Copies

OFFSITE

M. Mintz
U.S. Department of Energy
Division of MHD
FE-26, F-338, GTN
Washington, DC 20545

M. Covington
DOE Butte Project Office
P.O. Box 3462
Butte, MT 59701

F. Herbaty, Sr., MHD
DOE Chicago Operations Office
9800 S. Cass Avenue
Argonne, IL 60639

T. Arrigoni
Technical Project Officer
PM-20, Mail Stop 920-215
Pittsburgh Energy Technology
U.S. Department of Energy
P.O. Box 10940
Pittsburgh, PA 15236

H. F. Chambers
Chief, MHD Management Section
PM-20, Mail Stop 920-215
Pittsburgh Energy Technology
U.S. Department of Energy
P.O. Box 10940
Pittsburgh, PA 15236

J. O. Hunze
DOE Operations Office
University of Tennessee Space Institute
Tullahoma, TN 37388

27 DOE Technical Information Center

No. of Copies

M. Petrick
Argonne National Laboratory
9700 S. Cass Avenue
Argonne, IL 60439

W. Redman
Argonne National Laboratory
9700 S. Cass Avenue
Argonne, IL 60439

Mr. Roepke PWT/PT
AEDC Division
Arnold Air Force Station, TN 37389

L. Whitehead, Calspan
AEDC Division
Arnold Air Force Station, TN 37389

R. V. Kessler
AVCO Everett Research Laboratory
2385 Revere Beach Parkway
Everett, MA 02149

F. Hals
AVCO Everett Research Laboratory
2385 Revere Beach Parkway
Everett, MA 02149

A. C. Dolbec
Advanced Fossil Power Systems
Electric Power Research Institute
P.O. Box 10412
Palo Alto, CA 94304

R. J. Ferraro
Electric Power Research Institute
P.O. Box 10412
Palo Alto, CA 94304

D. DeCoursin
FluiDyne Engineering Corp.
5900 Olson Memorial Highway
Minneapolis, MN 55422

No. of Copies

R. Rhodenizer
General Electric Corp.
Research Laboratories
Schenectady, NY 12305

J. C. Cutting
Gilbert Associates, Inc.
P.O. Box 1498
Reading, PA 19603

A. Dawson
Massachusetts Institute of Technology/PFC
NW-16-130
Cambridge, MA 02139

D. Murphee
Mississippi State University
Aerophysics and Aerospace Engineering
P.O. Drawer A/AP
Mississippi State, MS 39762

J. Orth
Montana Energy and MHD R&D Institute
P.O. Box 3890
Butte, MT 59701

G. E. Youngblood
Montana Energy and MHD R&D Institute
P.O. Box 3890
Butte, MT 59701

R. Rosa
Montana State University
Department of Mechanical Engineering
Bozeman, MT 59715

J. Sherick
Mountain States Energy, Inc.
P.O. Box 3767
Butte, MT 59701

No. of Copies

J. Winters
NASA/Lewis Research Center
21000 Brookpart Road
Cleveland, OH 44135

S. Demetriades
STD Corporation
P.O. Box C
Arcadia, CA 91006

C. Maxwell
STD Corporation
P.O. Box C
Arcadia, CA 91006

C. H. Kruger
Stanford University
Palo Alto, CA 94305

M. Bauer
TRW, INC.
One Space Park
Redondo Beach, CA 90278

J. Hardgrove
TRW, INC.
One Space Park
Redondo Beach, CA 90278

M. A. Scott
University of Tennessee Space Institute
Tullahoma, TN 37388

S. Wu, Director
University of Tennessee Space Institute
Tullahoma, TN 37388

A. Jones
Westinghouse Electric Corporation
Waste Technology Services Division
P.O. Box 10864
Pittsburgh, PA 15236

No. of
Copies

FOREIGN

R. P. Indwar
Central Mine Planning and
Design Institute, Ltd.
Gondwana Place
Kanke Rd.
Ranchi 834008 India

ONSITE

DOE Richland Operations Office

H. E. Ransom

No. of
Copies

22 Pacific Northwest Laboratory

J. L. Bates
C. R. Hann
P. E. Hart
D. D. Marchant (10)
R. P. Turcotte
P. L. Whiting
Technical Information (5)
Publishing Coordination (2)